■Ngày nhận bài: 09/12/2024 ■Ngày sửa bài: 17/01/2025 ■Ngày chấp nhận đăng: 06/02/2025

ANSYS based analysis of low density rc slab with metal meshing

Phân tích sàn bê tông cốt thép có trọng lượng riêng thấp bằng mô phỏng số ANSYS

> MSC HUYNH HAN PHONG
Faculty of Civil Engineering, Mien Tay Construction University
Email: huynhhanphong@mtu.edu.vn

ABSTRACT

Shear failure of punching pertaining to slab of concrete reinforced type consisting of metal mesh expansion and lower density aggregates was simulated numerically in this study. We studied and spoke about the simulations' outcomes. Because punching shear failure occurs so suddenly and brittlely, research into it was crucial. Software of Finite element analysis (ANSYS V.2020.R1) was used for creating numerical models for punching shear failure of such slabs. Both non-linear performance of concrete and steel are considered for development of such prototypes. Modeled slabs applied solid components for concrete, space bars for reinforcements, a smear layer of embedded inside solidified elements for simulating an extended mesh of metal. Test information provided in concerned tasks were compiled by reviewing appropriate literature. Slab's Numerical prototypes were tested, and their findings compared to published experimental data utilizing load deviation responses and pattern of fracture. There was excellent aligning between experimental outcome and findings of computer models. Predictions concerning the punching resistance of concrete slabs reinforced with expanded metal mesh and concrete slabs built with low density aggregate may be generated using the numerical models created for this work.

Key words: Reinforced Concrete; ANSYS; Punching shear; Low density concrete; slabs; Ferrocement.

1. INTRODUCTION

When designing reinforced concrete slabs [1] that are exposed to concentrated loads or that are located around supported columns, it is known that the two-way reinforced concrete shear failure of flat slabs amongst major designing issues. Two-way shear failure is the root cause of the rapid brittle failure. Many scientists have tested both low-density and standard-density reinforced concrete slabs, as well as EMM-reinforced concrete slabs. These slabs have been exposed to many different environments [2].

Due to its exceptional strength to weight ratio, low density aggregate concrete (LDAC) may be employed in a wide range of applications. As determined by experimental analysis of LDAC slabs' punching shear behavior [3], the surface failure angle of punching shear is affected by the kind of low density aggregate used. Two kinds of low density aggregates were employed in the punching shear tests for this investigation. Higashiyama et al. [4] looked at the elements that reduced punching sheared strength of 5 low density reinforced concreted slabs, finding fact about density of aggregate fell, so did the punching shear strength.

Test experiment was conducted over connection of 3 slab-column connections with a combined length of 762 cm as structure of flat slab to compare performance of stud railings arranged in radial or orthogonal layout in slab-column junction whose slabs contains comparatively lower ratio of flexural reinforcements [5]. The connection of 3 slab-column totaling 7.62 m long were analyzed in this research. The shear strength of slab-column connections was found to be significantly improved by using a radial architecture as opposed to an orthogonal one. The researchers wanted to test the effects of high temperatures on low density silica fume aggregate concrete and found that increasing substitution proportion of silica fume aggregate improved working capability while decreasing compressive strength and density [6]. It was discovered that using pre-wetted low density aggregates as part of a novel strategy to internal curing increased hydration while decreasing cracking and shrinkage. The method was successful in achieving the desired result. With this method, water may be used for cement hydration at any time throughout the life of the concrete. Naama et al. [7] explain that ferrocement is a composite material used as a structural component due to its low price. Expanding wire mesh and cementitious mortar form the layers of this material.

In order to improve prefabricated foam concrete, which had a density ranging from 1300 to 1900 kg/m^3, Helal et al. [8] conducted a practical study to investigate the best ways to do so. This study made use of a water reduction agent in addition to two other types of materials that are added to concrete (fly ash and silica fume). The water reduction agent was the primary focus of the investigation. The outcomes of the research were promising since these materials showed a discernible improvement in the structure of the pores in concrete, in addition to an increase in strength and a reduction in the quantity of water that was absorbed by the concrete. In addition, the data suggested that the use of these materials resulted in a little rise in the level of heat conductivity shown by concrete. According to the findings of the study [9] conducted by Wan Ibrahim et al., the

compressive strength and flexural strength of foam concrete were evaluated in relation to the influence of polyolefin fibres. The density of the concrete that was used in this experiment ranged from 1300 to 1600 kg/m^3, depending on the exact mix. Polyolefin-sized fibres were employed by the researchers in the examination in quite modest volume fractions, with percentages ranging from 0% to 0.2%, 0.40% to 0.60%, respectively. The investigation was carried out in the United Kingdom. According to the results of the research, making use of the fibres stated above had a somewhat negative influence on the compressive strength and flexural strength of foam concrete, with a decrease of 4.3% and 9.3%, respectively. In addition, Lee et al. (2017) [10] used foam concrete slabs and beams in their study. These foam concrete structures had a density of 1700 to 1800 kg/m^3 and were created using a light foam mortar. As a direct consequence of this, the compressive strength of the concrete was 20 MPa. When compared to reinforced concrete with its natural density, the results of the research indicate that using the same sort of mortar resulted in a maximum load reduction of 8.0%, which brought the total reduction to 34.0%. According to studies and past study, the use of additives together with an assortment of fibre types might make foam concrete an effective material for usage in reinforced concrete structures. Slabs made of structural polystyrene foam concrete may be used in lieu of layers that provide thermal insulation and hollow block panels. However, the qualities and processes that went into the production of each design model for punching shear strength are quite different from one another [11-15]. A variety of design models have been developed for punching shear strength. Take, for instance, the semiempirical model known as the European Concrete Design Code (EC2) [16]. The FIB model design code, often known as MC [17], [18] is contrast-based in a physical sense. As a direct consequence of this, a number of studies have been conducted to investigate how flat slabs behave when exposed to fire [19]. Despite the diversity of these experiments, the behaviour of polystyrene foam concrete when it is subjected to fire was not investigated. In their experiment, El-Fitiany and Yousef [20] employed a simple method to make a prediction about the behaviour of reinforced concrete sections when they were subjected to high temperatures.

2. MATERIALS AND METHODS

2.1. Material Properties

Table 1 provides the volume % of the wire mesh together with the material parameters of the modeled slabs derived from the literature. Mechanical features of concrete used are provided in table with group ID and the slab thickness. Compressive strength, tensile strength, and elasticity are all examples of these characteristics.

Table 1: Cementitious slabs and modeled concrete features of material

Group	Specimen	Thickness mm	Compressive strength f_c' (MPa)	Tensile strength f_{sp} (MPa)	Modulus of Elasticity E_c (GPa)	Volume fraction v_f	Reference
1	NN	200	40.6	3.41	31.7	---	Youm et al. (2014)
	LA	200	37.2	3.40	22.6	---	
	LD	200	34.2	2.82	20.0	---	
2	Slab-I	40	32.0	5.20	24.9	---	Ibrahim, (2011)
	Slab-Ø6	50	32.0	5.20	24.9	1.41	
	DP-2.0	50	32.0	5.20	24.9	0.60	

Table 2, lists the bars that were utilized in the Slab-6 specimen that was created by Group 1 and the DP-2.0 specimen that was created by Group 2.

Table 2: Feature of steel bar material used

	Ø10 mm steel bars	Ø6 mm steel bars
Yield stress	411 MPa	252 MPa
Ultimate strength	600 MPa	364 MPa
Elongation	12 %	30 %
Elastic modulus	200 GPa	195 GPa

Expanded metal mesh (EMM) material features used for creation of DP-2.0 specimens for Group 2 are detailed in Table. 3.

Table 3: Expanded metal mesh (EMM) material features used

Diamond size	22.5x57.5 mm
Dimension of strand	2 mm
Proof stress	300 MPa
Proof strain	0.117%
Ultimate strength	500 MPa
Ultimate strain	5.4%

2.2. Concrete Slabs simulation details

Youm et al. (2014) report that the first group included one normalized weight concrete slab (NN) with 2 low density concrete slabs (LD and LA). Size and reinforcing layout of the three slabs were identical. Dimensions of the slabs and reinforcement placements are shown in Figure 1. The thickness of the top and bottom layers was 20 m. The vertical movement was achieved with the help of 300 mm square, 35 mm thick steel plates.

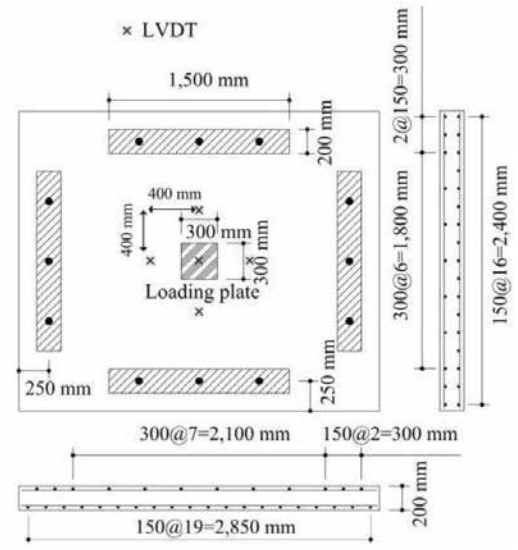

Fig. 1. Illustration showing NN, LA, and LD samples

Approximately 27 cementitious 490 mm by 490 mm x 40–60 mm thick square slabs made comprised the second set, as stated by Ibrahim (2011). This arrangement relied on the edges of the slabs for support. Three specimen models were developed throughout this investigation: Slab-I, Slab-6, and DP-2.0. Simple mortar was used in the early construction of the slab. The second slab was made of cementitious material, had a thickness of 100 mm, and was reinforced by steel bars 6 mm in diameter running in opposite directions. The third example is a 2-millimeter-thick cementitious slab that has been reinforced with an EMM ferrocement layer. A steel plate, 80 millimeters square and 20 millimeters thick, was used to apply the vertical displacement.

Dimensions of the slabs and the different reinforcing arrangements are shown in Fig. 2.

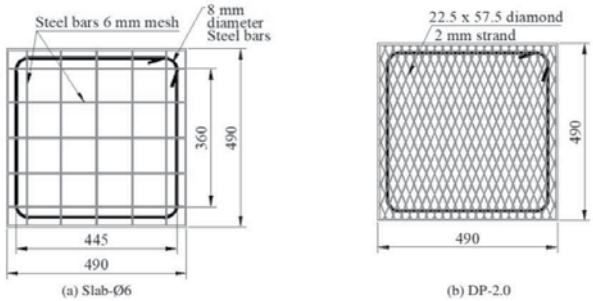

Fig. 2. Dimensions of the specimens with reinforcements

2.3. Model of Finite Element

Developed FE prototype were constructed using plans of experiment as their foundation [10]. In this part, we'll go through the methodology used by the subsequent models of finite element we suggest.

Ferrocement layer, Reinforcement grid and Concrete:

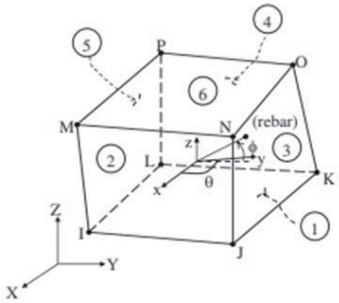

Fig. 3. Details on the Solid65 element's shape, node positions, and coordinate system

The robust nonlinear analytical capabilities of ANSYS V.2020.R1 were employed for the modeling of all slabs. All six scenarios (NN, LA, LD, Slab-I, and Slab-6) were modeled with the help of ANSYS's algorithms.The solid65 sub-element concerning given finite element models represented actual concrete. A solid element in three dimensions, Solid 65 includes eight nodes and 3 freedom degrees (translated in x, y, and z axes) on every node, as shown in Figure No. 3. This means that Solid 65 may shift in any of the aforementioned three ways. Nonlinearities in materials and geometry, as well as cracking under tension and crushing under compression, may all be modeled using this element. In addition, it may represent the crushing effect of stress. Additionally, it is capable of imitating fear. A smudged layer that was concealed among solid parts was used for the aim of imitating the EMM layer. Open cracks were given a shear transfer coefficient of 0.3, whereas closed cracks were given a 0.6 value. The shear transmission in fractured concrete components was evaluated using these two values.

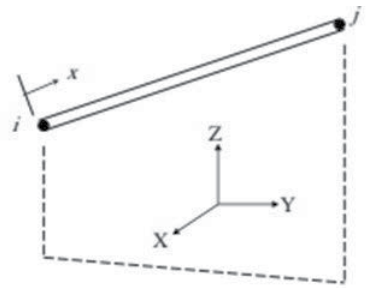

Fig. 4. The Link8 element's shape, node locations, and coordinate space.

Fig. 4 demonstrates how the Link8 element were deployed in simulating reinforcement grid pertaining to non-ferrocement layer samples. Uniaxially loaded throughout its length, Link8 is a space bar element having 3 degrees of freedom (z, x and y) at every nodal junction. Link8 may be used to recreate the effects of large deformations and the nonlinearity of materials. Fig. 5 depicts a reinforcement bar model, while Fig. 6 shows a solid-component concrete mesh.

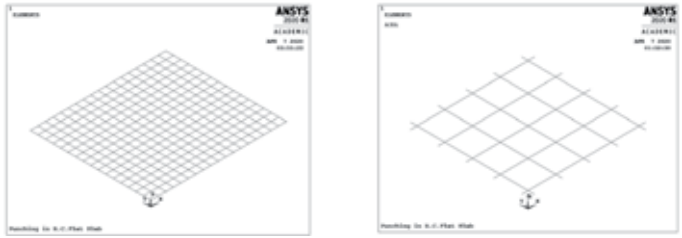

Fig. 5. we see the mesh components (link8) utilized to create the reinforcement grid

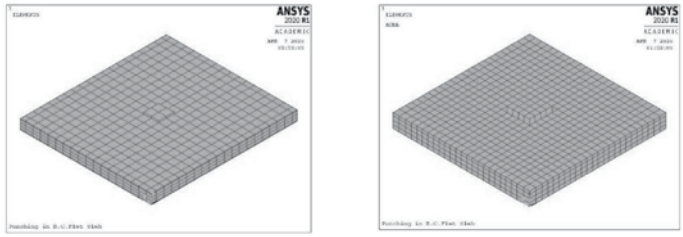

Fig. 6. Mesh components with a solidity level of solid65 to represent cementitious and concrete slabs

Plastic deformation and modeling Material properties

The stress-strain curve for group 1 specimens reinforced with steel bars of diameter less than 10 millimeters is shown in Fig. 7. The strain-stress relation for concrete is showcased through Fig. 8 using LA specimen as the data point. The Poisson's ratios for concrete were established at 0.2 and those for steel at 0.3. These criteria were consciously chosen as the best fit.

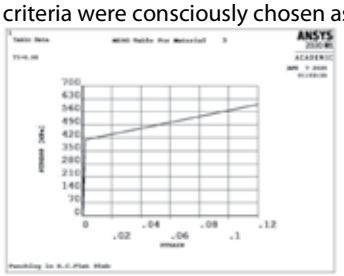

Fig. 7. For steel bars with a diameter of 10 millimeters, the stress-strain curve

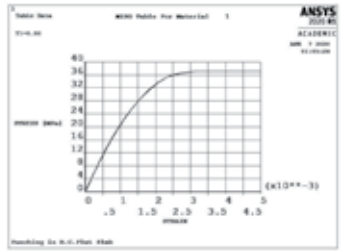

Fig. 8. The stress-strain relationship for recycled concrete (fc' = 37.2 MPa)

Loading and boundary conditions:

To mimic the experimental work under circumstances analogous to when the slabs were simply supported, translational restrictions in the x, y, and z directions were added as boundary conditions at the four corners of the slabs. The top surface of the loading plate was displaced vertically in the direction of a negative Z in order to mimic the real loading operation. Every joint was treated in this way. You can see the four-corner boundary conditions with used displacements concerning to first groups in Fig. 9, for second group in Fig. 10. The two pictures may be found in the same file.

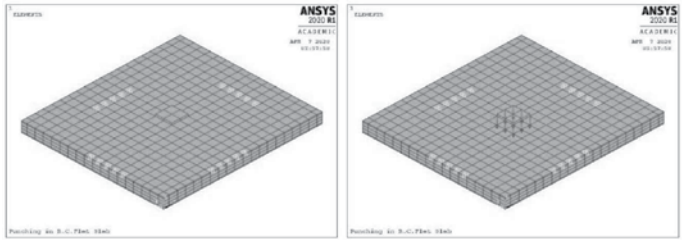

Fig. 9. The constraints and the amount of displacement that was applied to the first group

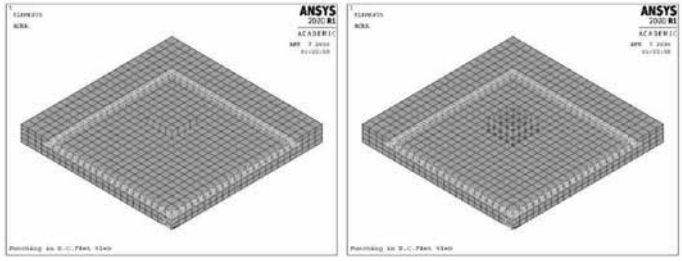

Fig. 10. Second group's applied and Restraints displacement pertaining to secondry group

Analysis of Non-linear nature:

Automated stepping of time were utilized as a means of regulating non-linear resolution due to non-linear character of issue under consideration. Using a thorough implementation of the Newton-Raphson technique, the non-linear equations were solved. To regulate the convergence of non-linear solution, force of residual convergence criteria got applied, and an appropriate tolerance has been given to it.

Bond behavior

People believed the connection between the reinforcing bars and the concrete was excellent because they assumed bond failure did not play a role in slab collapse. In other words, the expected load at failure and the deformed shape are not likely to be significantly affected by the underlying premise of this inquiry.

3. RESULTS

The results from each sample are summarized in Table 4. Fig. 11 provide both numerical and experimental results for the maximum loads that may be applied to members of group 1. Fig. 12 illustrate both numerical and experimental examples of the maximum loads that may be applied to Group 2 members. Center deflections at ultimate loads for Group 1 are calculated using both experimental and computational methods. Fig. 13 displays these findings. Center deflections under maximum loads applied to Group 2 are shown for both theoretical and experimental methods in Fig. 14.

Table 4: A comparison between the computational and experimental data for the maximum load and the central deflection.

Group	Specimen	Experimental results [1,8]		Numerical Results		Numerical/Experimental	
		Max. load (KN)	Deflection (mm)	Max. load (KN)	Deflection (mm)	Load	Deflection
1	NN	670.4	16.7	675.64	16.67	1.008	0.998
	LA	552.0	10.6	556.63	11.28	1.008	1.064
	LD	626.3	15.2	605.96	14.80	0.968	0.974
2	Slab-I	8.0	0.32	8.60	0.34	1.075	1.063
	Slab-Ø6	34.5	6.2	34.77	6.0	1.008	0.968
	DP-2.0	25.0	4.5	26.30	4.25	1.052	0.944

Figs 15–20 presents experimental as well as numerical respnses of load-deflection responses over central points of six investigated slabs. Calculated findings and the experimental data were in close agreement. For failure loads and maximum deflections, the numerical and experimental values were off by around 8% and 7%, respectively. The provided models thus provided reliable predictions of failure load and displacement.

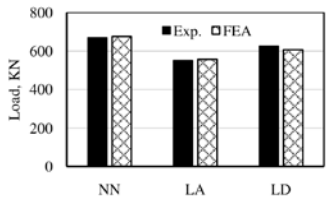

Fig. 11. The FEA and experimentally calculated ultimate load for group 1.

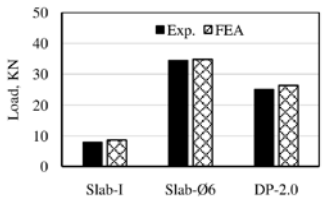

Fig. 12. The ultimate load for group 2 (Finite Element Analysis vs. Experimental Data).

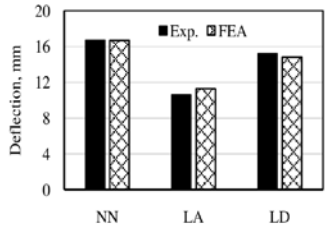

Fig. 13. The central deflection from the FEA-testing.

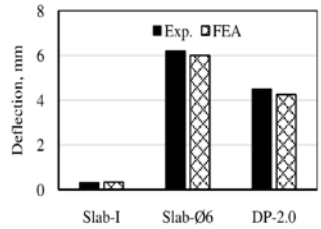

Fig. 14. The results of a comparison, FEA-experimental data with regards to the central deflection.

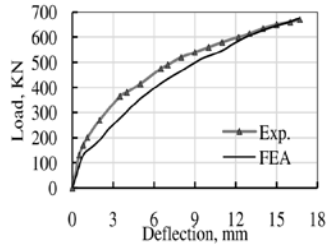

Fig. 15. The NN slab's load deflection response

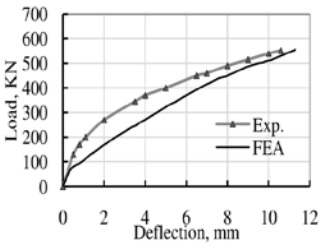

Fig. 16. The load deflection response of the LA slab

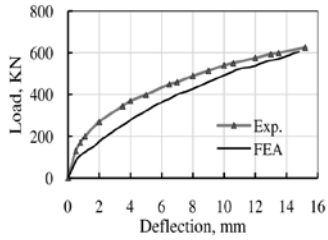

Fig. 17. The LD slab's load-deflection response

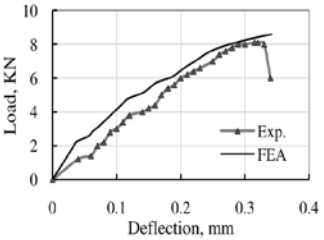

Fig. 18. The load deflection response for Slab-I

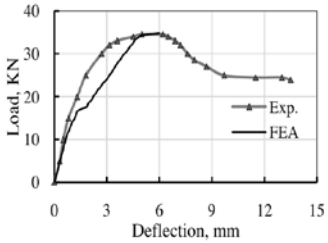

Fig. 19. The load-deflection response of Slab 6

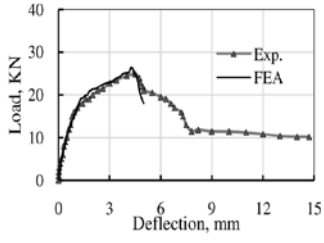

Fig. 20. The DP2.0 slab's load-deflection response

The discrepancies between the numerical and experimental failure patterns are graphically shown in Fig. 21. And Fig. 22 shows how the warping affects the form of the LA, LD, and DP-2.0 slabs. Computational outcomes was quite close to testing observations.

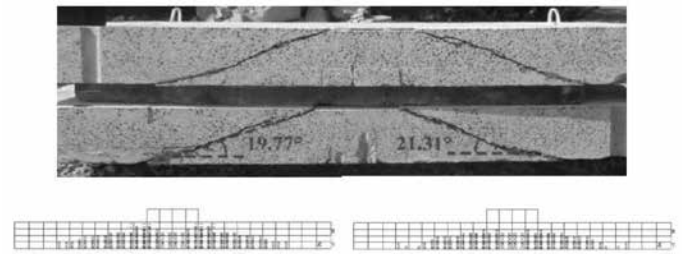

Fig. 21. Depicts patterns of failure for LD and LA slabs as shown in the experimental and FE models.

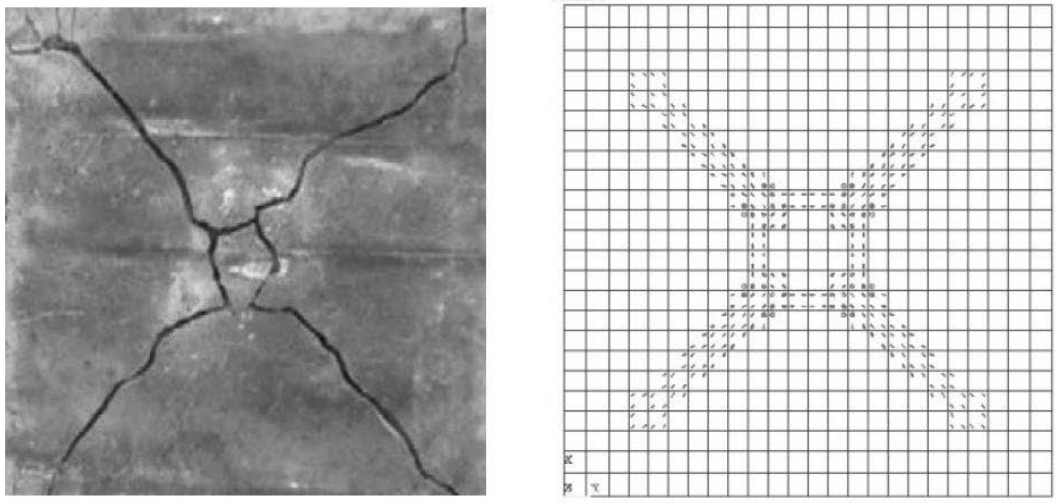

Fig. 22. Depicts the failure pattern for the DP-2.0 slab that was seen experimentally and was predicted by the FE models.

4. CONCLUSION

In this research, a finite element model built in ANSYS is used to provide predictions about shear response of punching with strength of several slab types. Cementitious slabs with reinforcement (a regular bar's grid or layer of ferrocement), cementitious slabs having no reinforcement (without reinforcement). Six concrete slabs were subjected to a three-dimensional FEA with a nonlinear analysis. Based on the algorithms given in [11] and [18], finite element models were developed and tested, with the results compared to those from the experiments. Failed loads, deformed forms, center deflections at ultimate loads, , pattern of failure was all very close to predictions. Analysis of Non-linear finite element is a powerful software on studying response of concrete and cementitious slabs under punching shear. Given finite element prototype may be useful software in forecasting shear resistance of punching for kinds of slabs mentioned, reducing need for expensive trials. As a result, it is now possible to conduct a thorough numerical analysis of shear punching performance and factors affecting shear strength of punching. In the past, this was not the situation.

REFERENCES

[1]. Okasha, Mostafa Ali Taha Ali, et al. "Analysis of lightweight composite sections with reinforced concrete infill with autoclaved aerated concrete (AAC)." Frontiers in Built Environment 9 (2023): 1149442.

[2]. Islam, Sheikh Ubair Ul, Avani Chopra, and Aditya Kumar Tiwary. "Finite Element Analysis of High-Strength Concrete Pavement Made With The Addition Of Fibres." IOP Conference Series: Earth and Environmental Science. Vol. 1110. No. 1. IOP Publishing, 2023.

[3]. Kozarić, Ljiljana, et al. "Experimental investigations and numerical simulations of the vibrational performance of composite timber-lightweight concrete floor structures." Engineering Structures 270 (2022): 114908.

[4]. Jain, Nikita, and Asif Hussain. "Numerical Analysis on Different Void Former On ANSYS." IOP Conference Series: Earth and Environmental Science. Vol. 796. No. 1. IOP Publishing, 2021.

[5]. Madan, Chinnasamy Samy, et al. "Influence on the flexural behaviour of high-volume fly-ash-based concrete slab reinforced with sustainable glass-fibre-reinforced polymer sheets." Journal of Composites Science 6.6 (2022): 169.

[6]. Martínez-Martínez, Juan Enrique, et al. "Nonlinear Thermo-Structural Analysis of Lightweight Concrete and Steel Decking Composite Slabs under Fire Conditions: Numerical and Experimental Comparison." Applied Sciences 12.18 (2022): 9306.

[7]. Naama et al. "Analysis of a Ribbed Slab without Reinforcement using ANSYS." i-Manager's Journal on Structural Engineering 11.2 (2022): 31.

[8]. Helal et al. "Analysis of Lightweight Polystyrene Foam Concrete Flat Slabs under Fire Condition." Advances in Civil Engineering 2022 (2022).

[9]. Wan Ibrahim et al. "Simulation of structure and power generation for Self-Compacting concrete hollow slab solar pavement with micro photovoltaic array." Sustainable Energy Technologies and Assessments 53 (2022): 102798.

[10]. Lee et al. "Comparison of the flexural behavior of high-volume fly ashbased concrete slab reinforced with GFRP bars and steel bars." Journal of Composites Science 6.6 (2022): 157.

[11]. Madiwalar, Sahana S., R. Subash Chandra Bose, and Shiva Shankar KM. "Analysis of Composite Beam with Shear Connectors Using FEA Software (ANSYS)."

[12]. Lyu, Ping, et al. "Explosion test and numerical simulation of coated reinforced concrete slab based on blast mitigation polyurea coating performance." Materials 15.7 (2022): 2607.

[13]. Boushi, Abdulaziz, and Sepanta Naimi. "Optimization of Hollow Core Slab Strength Based on SFRC Orientation." Mathematical Modelling of Engineering Problems 10.1 (2023).

[14]. Al-Graishi, Shakir. Investigation of shear strength behavior of two-way slab panels based on different sfrc and heat effect. MS thesis. Altınbaş Üniversitesi/Lisansüstü Eğitim Enstitüsü, 2021.

[15]. Avci, Onur, and Ashish Bhargava. "Finite-element analysis of cantilever slab deflections with ANSYS SOLID65 3D reinforced-concrete element with cracking and crushing capabilities." Practice Periodical on Structural Design and Construction 24.1 (2019): 05018007.

[16]. Shaikh, Mohammad Farhan, and K. Nallasivam. "Static analysis of box-girder bridge under the influence of Indian railway vehicle loading using ANSYS finite element model." Advances in bridge engineering 3.1 (2022): 25.

[17]. Yang, Kailin, and Guangxiu Fang. "ANSYS Analysis of Prefabricated Light Aggregate Concrete Slab with Grouting." IOP Conference Series: Earth and Environmental Science. Vol. 237. No. 5. IOP Publishing, 2019.

[18]. Assad, Maha, et al. "Heat Transfer Analysis of Reinforced Concrete Walls in ANSYS and ABAQUS: A Comparative Study." 2022 Advances in Science and Engineering Technology International Conferences (ASET). IEEE, 2022.

[19]. Siddiqui, Shahida Anusha, et al. "Stability Analysis of a Cantilever Structure using ANSYS and MATLAB." 2021 2nd International Conference on Intelligent Engineering and Management (ICIEM). IEEE, 2021.

[20]. El-Fitiany and Yousef "Research Article Analysis of Lightweight Polystyrene Foam Concrete Flat Slabs under Fire Condition." (2022).